

A REVIEW PAPER ON NICKEL BASED ALLOYS FOR FINDING WELDING STRENGTH BY USING FRICTION STIR WELDING

Mrs P.Varalakshmi¹, K.Upendar², M.Priya Ranjani³, N.Rajesh Goud⁴, P.Arshad Khan⁵

Department Of Mechanical Engineering, Guru Nanak Institute Of Technology

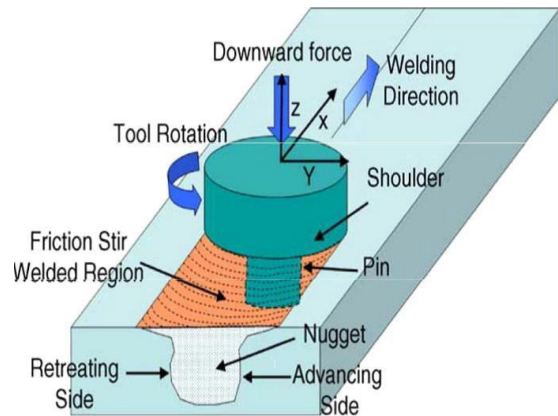
Ibrahimpattanam, Ranga reddy Dist, India.

Abstract

A nickel base (Ni-base) alloy is one that has nickel as its primary constituent. These alloys have found usage in a variety of industries, such as aerospace, petroleum, chemical, and power generation industries. The alloys have been used in a variety of demanding environments from cryogenic to very high temperatures, fresh water and salt water to acidic solution containing vessels, steam and pressure vessels to electronic and biomedical components. It is evident that a wide variety of Ni-base alloys with different properties can be engineered for nearly any application. During friction stir welding (FSW), the tool plays a major role in this solid state joining process, heating, softening and moving the work piece material from the advancing side of the tool to the retreating side joining the two plates or sheets together. In FSW of high temperature materials such as steels, titanium and Ni based alloys becomes feasible whenever a suitable FSW tool material is available.

INTRODUCTION

FRICTION STIR WELDING (FSW) was firstly invented in 1991 at the Welding Institute (TWI) of the United Kingdom as a solid-state material joining process and this was initially applied to aluminium alloys. The basic of friction stir welding working is simple a non-consumable rotating tool with a specially designed pin and shoulder is inserted into the abutting edges of two plates to be joined and subsequently traversed along the joint line. Definitions for the tool and work piece Advancing and retreating side orientations require to tool rotation and travel directions.



Friction stir welding diagram

The process parameters are:

S no.	Parameters	Effect of parameters
1	Rotational Speed	Frictional heat, stirring, oxide layer breaking and mixing of material
2	Welding Speed	Appearance and heat control.
3	Tilting Angle	appearance of the weld, thinning

Tool materials

Tool material characteristics are also critical for FSW. The tool material depends on the work piece material and the desired tool life as well as the user's own preference. The tool material should have the following properties such as:

- (i) Higher compressive yield strength at elevated temperature than expected force forces onto the tool.
- (ii) It should have Good strength, dimensional stability and creep resistance
- (iii) Good thermal fatigue strength to resist the repeated heating and cooling cycles

(iv) There is no harmful reaction with the work piece material

(v) There should be good fracture toughness to resist the damage during plunging and dwelling

(vi) Low coefficient of thermal expansion between the probe and the shoulder materials to reduce thermal stresses.

(vii) Good machinability to ease manufacture of complex features on the shoulder and probe

(viii) Low cost.

Tool materials and suitable weld metals:

Tool Material	Suitable weld material
Tool steels	Al alloys, aluminum metal matrix composites (AMCs) and copper alloys
WC-Co	Aluminum alloys and mild steel
Ni-Alloys	Copper alloys
WC composite	Aluminum alloys, low alloy steel and magnesium alloys, Ti-alloys
W-alloys	Titanium alloys, stainless steel and copper alloys
PCBN	Copper alloys, stainless steels and nickel alloys

1. Machinability of nickel-base super alloys

Author: I.A. Choudhary

Super alloys are heat-resistant alloys of nickel, nickel-iron, or cobalt that exhibit a combination of mechanical strength and resistance to surface degradation generally unmatched by other metallic compounds.

conclusion: Flank wear of the whisker-reinforced alumina and silicon tools can be considered as a diffusion type wear. Alumina-TiC ceramic tools are best suited for high speed machining (over 400 m min⁻¹) or high feed rate, whilst whisker-reinforced alumina suitable for a medium cutting speed (100–400 m min⁻¹) with a low feed rate. Uncoated carbide tools are better than the coated tools for machining Inconel 718.

2. Friction Stir Welding of Austenitic NiTi Shape Memory Alloys

Author: Lima, J. S.

Materials and tools: Austenitic NiTi shape memory thin sheet was used in the FSW the process parameters used was 180 mm/min welding travel speed and rotation of tool tip of 1500 rpm. The tool shoulder diameter is 17 mm and the tip diameter is 2mm. Tensile tests were performed on an MTS 810 testing machine with a displacement rate of 0.05mm/min at a room temperature. The fracture surfaces were observed by scanning electron microscopy (SEM) by using a TESCAN microscope.

Conclusion: Thin sheets of NiTi SMA were welded by FSW process. The welded joint obtained by this process presented good mechanical properties and it was capable of achieve 700MPa Ultimate tensile strength, and 13% strain. The welded joint remained in the austenitic phase state. In FSW the welded portion have high strength compared to fusion welding process. The stress induced martensite occurs at 450 MPa in the welded condition, Which is 50MPa above the base metal. The increase in mechanical resistance in detriment of ductility was observed and indicates that hardening occurs in function of the mechanical work of the friction stir welding process.

3. Friction stir processing of Ni-base alloys:

Author: J C Lippold

Friction stir processing (FSP) is a materials processing technique is that a derivative of friction stir welding (FSW), where a non-consumable rotating tool consisting of a shoulder and pin is plunged into and translated across the surface of a work pieces. A homogenous, fine grained microstructure generally results due to the combined thermal and mechanical effects are analogous to material forging.

Materials and tools: The compositions of the plate material and filler metal (Alloy 282) used. FSP experiments, Hast alloy X, Alloy 625, and Alloy 718 plates were cut into 75 * 150 mm pieces. FSP was conducted using a W-25Re tool with dimensions. K thermo couples to record thermal histories during processing. 180 RPM/0.85 mm/sec for Hast alloy X

100 RPM/1.05 mm /sec for Alloy 625, and 100 RPM/0.85 mm /sec for Alloy 718.

conclusion : Processing ranges are in terms of spindle rotation and travel speed were established all three alloys with Alloy 625 exhibiting the largest processing window and Alloy 718 the smallest. Tool wear was observed for all three materials and is found on the advancing side of stir zone. Temperatures histories were successfully recorded for settings central to the processing window with peak temperatures for Hast alloy X and Alloy 625 of 1150°C and 1100°C for Alloy 718.

4. Friction stir welding on Monel alloy at different heat input conditions microstructural behaviour and tensile behaviour:

Author: Akbar Haiderzaeidh

Materials and tools: 2 mm thick Monel 400 plates were friction stir welded at different heat inputs. For the low and high heat input conditions, the tool rotational and traverse speeds were, respectively, 450 rpm/¹ 900 rpm/25mmmin⁻¹. A WC-Co tool consisted of a ø12 mm shoulder and a pin of ø3*1.75mm was employed. The peak temperature was measured during FSW using K type thermocouples inserted into the back side of the plate. Microstructure of the joints was characterized using orientation imaging microscopy (OIM) with a step size of 70 nm at different microstructural zones. For studying the tensile properties, specimens were prepared according to ASTM-E8 M standard, and then the tensile tests were carried out at a strain rate of 1 mm min⁻¹.

conclusion : The heat input amount has an extensive effect on microstructure evolution during FSW and the mechanical properties of the Monel. At low heat input condition, DDRX and CDRX result in the formation of fine grains with a large amount of HAGBs and a nearly random texture. At high heat input condition, CDRX causes large grown grains with a shear texture. The low heat input condition results synergic increase of the strength and elongation. Finer grain size, larger Taylor factor, more HAGBs and random

texture of the SZ are the main reasons of the better tensile behaviour of the low heat input joint.

5. High-resolution EBSD characterisation of friction stir welded nickel–copper alloy: effect of the initial microstructure on microstructural evolution and mechanical properties:

Author: Akbar Heidarzadeh

Materials and tools: The BM's used in this study were the Monel 400 (about 67% Ni–23% Cu) sheets with a thickness of 2 mm. Two different types of annealed and rolled BM's were selected to investigate the effect of initial condition on the microstructural and textural evaluation during FSW. The FSW tool was made of WC-Co, which was made a pin of ø3×1.75 mm, and a shoulder with a diameter of 12 mm. For the both joints, the tool rotation speed and welding speed were set constant at 900 rpm and 25 mm/min, respectively. For the microstructural and textural study, electron back-scattered diffraction (EBSD) technique was used for orientation imaging microscopy (OIM).

Conclusion: The effect of initial conditions of Monel 400 BM's on the microstructure, texture components and strength of the different zones of the friction stir welds was investigated using high-resolution EBSD and Vickers hardness test. When the Monel 400 alloy with an annealed structure is friction stir welded, the grain growth in HAZ, DRV and CDRX in TMAZ, and pure CDRX in SZ occur. These mechanisms cause a lower fraction of HAGBs, larger grains, and higher texture intensity in the final structure of the joint. On the other hand, in the case of the Monel 400 alloy with an initial rolled structure, SRX in HAZ, and CDRX and DDRX in TMAZ and SZ of the joints are the key mechanisms, governing the microstructural evolution during FSW. The higher contribution of the DDRX causes the formation of a higher fraction of HAGBs, finer grain sizes, higher dislocation density, and higher texture intensity in the final microstructure of the joint. Therefore, it is better to choose the Monel 400 BM with an initial rolled structure for FSW because the strength of the joint will be improved by grain boundary and dislocation strengthening mechanisms.

6. Shape Memory Effect, Temperature Distribution and Mechanical Properties of Friction Stir welded nitinol:

Author: S.S. Mani Prabu

Materials and tools: Austenitic NiTi sheet of 1.2 mm thickness with Ni 50.75. % was used for welding. The sheets were cut into dimensions 50 mm × 70 mm and welded using five-axis FSW machine (BISS ITW Bangalore) in closed square butt configuration. Three rotational speeds (800 rpm, 1000 rpm and 1200 rpm) with constant traverse speed of 50 mm/min in the ambient environment without any cooling medium or shielding gas. A tungsten alloy tool was used for welding. The samples for microstructural analysis were polished using various grits of SiC paper, then using alumina powder and finally etched using 50 mL H₂O + 40 mL HNO₃ + 10 mL HF solution. The microstructures were recorded and using Carl Zeiss inverted optical microscope.

Tensile test samples with a cross section of 1.2 mm × 4 mm were machined across the weld. Tensile test was carried out on Instron-5967 machine at a strain rate of 10⁻³. Vickers microhardness measurements were taken along the cross section of the weld using the FM-800 Future Tech Corp at 500gf load at 15 seconds. The characterization techniques to evaluate the microstructures, phases, hardness and stress-strain behaviour were performed at the room temperature.

A strip of dimension 65 mm × 2 mm × 1.2 mm was cut across the weld and used for actuation studies.

Conclusion:

Welding processes are currently inevitably applied to Ni alloys, particularly used in the oil and gas industry, and friction stir welding represents a convenient alternative for the problems that typically occur in conventional fusion welding processes. The relatively slow occurrence of microstructure transformations in Ni base alloys enable the achievement of an as welded microstructure similar to the annealed state, especially for solid-solution alloys, and grains recrystallized to a grain size often smaller than that of the BM.

7. Effect of friction stir welding speed on mechanical properties and microstructure of nickel based super alloy Inconel 718:

Author: Z. Ahmed

Materials and tools: 4 mm thick nickel based super alloy Inconel 718 has been friction stir welded using different traverse speeds of 30, 50 and 80 mm/min at a rotation rate of 400 rev/min. Since the Inconel 718 alloy was friction stir welded in the annealed condition, a significant increase in mechanical properties has occurred. Microstructural evolution in the nugget (NG) zone has been investigated using electron back scattering diffraction (EBSD) at the top surface and near the base of the NG as well as across the transverse cross-section of material.

Conclusion: The FSW of 4 mm thickness Inconel 718 alloy is feasible by using a silicon nitride tool. The mechanical properties have significantly improved after FSW mainly due to grain refining and precipitation in NG region. Hardness has increased in the NG region relative to the base material, and the tensile properties after FSW were still within the range of the annealed properties of alloy. In addition, FSW has resulted in a significant reduction in grain size across the transverse cross-section from the base material to the NG region. In addition, sharp variation in the grain size has resulted along the thickness of the weld in the NG from 5 mm near the top to 2 mm near the base of the NG. The increase in FSW speed has resulted in more reduction in grain size and enhances the hardness values.

8. Corrosion properties of friction-stir processed cast NiAl bronze:

Author: D.R. Nia

Materials and tools: Experimental

Commercial UNS C95800 NAB alloy (chemical. %: Al 9.18, Ni 4.49, Fe 4.06, Mn 1.03, Cu balance) cast plates with dimension of 300 mm × 70 mm × 8 mm were subjected to FSP under a tool rotation rate of 1200 rpm and a traverse speed of 50 mm/min with a tool tilt angle of 3°. A nickel-based alloy tool with a concave shoulder 24 mm in diameter, and a

threaded conical pin 8 mm root diameter and 7 mm in length was used. Both the tool and the processed workpiece were subjected to blow over cooling during FSP. The microstructure of the cast and FSP samples were examined using optical microscopy (OM) after etching with solution of 5 g FeCl_3 + 2 ml HCl +95 ml $\text{C}_2\text{H}_5\text{OH}$.

Static immersion samples were machined from the SZ with a dimension of 7 mm*7 mm*5 mm and were ground with 1000 Si C abrasive paper provide a uniform surface finish. Prior to test, the samples were degreased in acetone and blow-dried, and weighed carefully. Fifteen samples were suspended by the thin threads, and immersed into a tank containing 10 L of a 3.5 wt. % NaCl solution at room temperature. The solution was prepared from distilled water and reagent grade chemicals. The corroded samples were taken out after 24, 48, 96, 192, and 384h, respectively. The corroded samples were flushed with water and immersed in the solution of 500 ml HCl (density, 1.19) + 1000 ml H_2O for 2 min to clean off the corrosion products, then completely rinsed out using a toothbrush and flushed with water then immersed in alcohol and blow-dried, and finally weighed. For the purpose of comparison, the cast samples with the same size were tested under the same conditions. Corrosion surfaces were examined under an optical microscope (OM) and a scanning electron microscope (SEM), and furthermore, part of corrosion specimens were mounted, polished, and examined under a SEM.

Microstructure:

The optical cross-sectional macrograph of the FSP NAB. The microstructure of the cast sample was composed of coarse α phase, martensite β' phase, fine γ phase particles, and casting porosities. The light-etching phase with a size of 150 μm was the α phase, whereas the dark-etching constituents are associated with the various β transformation products.

conclusion :

The FSP sample showed much lower corrosion rate in the static immersion corrosion condition than cast sample due to the optimization of the microstructure

such as the refinement of grain size, elimination of casting porosities and segregation. The weight loss rate of both the cast and FSP samples decreased as the corrosion time increased at the first stage, and then gradually reached a steady level. The FSP sample showed slightly lower corrosion potential and a little bit higher corrosion current density. The slightly lower electrochemical corrosion resistance of FSP sample was ascribed to the existence of residual stress increased dislocations.

9. Laser-assisted friction stir processing of IN738LC nickel-based superalloy: stir zone characteristics

Author: S. M. Mousavizade

Materials and tools: The alloy used in this was an as-cast IN738LC nickel-based superalloy with the following composition (wt.-%): 0.10 C, 15.50 Cr, 9.8 Co, 3.04 W, 2.27 Mo, 0.70 Nb, 0.09 Fe, 4.36 Al, 3.15 Ti, 1.81 Ta, 0.04 Zr, 0.01 B and balance nickel, as determined by using a standard spark emission spectrometer (quant meter). The FSP and LAFSP were performed on 5.5 mm thick plates using a load-controlled FSW machine. Tungsten carbide-based alloy tools with shoulder diameter 15 and 6 mm probe diameter were used. The probe length was 1.2 mm and the tool axis was inclined 3° opposite to the direction of the tool advance. The tool rotation speed of 600 rpm, travelling speed of 50 mm min^{-1} and constant force of 30 KN were used for both the FSP and LAFSP. The specimens were sectioned transverse to the FSP direction and the microstructures of different zones were examined by optical microscopy (OM), scanning electron microscopy (SEM) and orientation image microscopy (OIM).

conclusion : Laser heating was used as a means for improving the FSP of a nickel-based superalloy (IN738LC). The stirring action results in significant grain refinement, precipitation of fine gamma prime and breakup of MC carbides of the base metal. Compared with FSP sample, LAFSP sample exhibited coarser grain structure with lower volume fraction of partially dissolved γ' precipitates in the centre and bottom of the SZ. The lower torque imposed on tool during LAFSP confirms improving

materials flow due to preheating effect of laser melting of a localised area ahead of FSP rotating tool.

10. Effect of plunge depth on microstructure and mechanical properties of FSW lap joint between aluminium alloy and nickel-base alloy:

Author: Qi Xian Zheng

Materials and tools: The materials used in this were Inconel 600 alloy and 2A70 aluminium alloy. Both materials were received as a sheet with a thickness of 2 mm. Each plate was degreased with methanol solvent followed by light sanding of plates to remove oxide and impurities. In this case, a WC-13%Co tool with a shoulder 18 mm in diameter and 2 mm long threaded conical pin. The tool-pin was tapered from the root diameter of 5 mm to the top diameter of 4 mm. During the FSW process, the 2A70 aluminium alloy was placed over the Inconel 600 nickel based alloy. FSW was performed at a tool rotation speed of 600-1200 rpm under the same traverse speed of 40 mm/min, plunge depth of 0-0.5 mm, and welding tool tilt angle of 2°. To prevent oxidation of the welded surface, argon shielding gas was utilized. The microstructure and shape of the cross section of weld joints were observed by optical microscopy after they had been mechanically polished and etched respectively (the aluminium side was etched with Keller's reagent and the nickel based alloy was etched with HCl+HNO₃). Using scanning electron microscopy (SEM) and X-ray diffraction (XRD), the more delicate structure and chemical compositions were analysed. The mechanical properties of FSW samples were evaluated at ambient temperature by Vickers microhardness and shear tests. The microhardness distribution in the cross-section of weld joints was measured perpendicular and parallel to the interface using an HXS-1000 microhardness tester with a load of 9.8 N and tested at a rate of 2 mm/min using Instron-5581 electromechanical testing machine at room temperature. Sound welds were achieved. When the tool pin reached the surface of the Inconel 600 alloy, the Ni alloy was shattered into pieces, resulting in non-uniform distribution of Ni alloy particles on the Al side. As the depth increased, the particles increased in size and quantity. Zones with

fine grains on the Ni side manifested higher hardness.

conclusion : Sound welds were achieved. When the tool pin reached the surface of Inconel 600 alloy, the Ni alloy was shattered into pieces, resulting in non-uniform distribution of Ni alloy particles on Al side. As the depth increased, the particles increased in size and quantity. Fine-equiaxed grains were found on the Al side, resulting from recovery and recrystallization during the FSW process. The grains in the SAZ were smaller than grains in the WNZ and TMAZ. A fine-grained zone also existed on Ni side and expanded as the plunge depth grew. The Zones with fine grains on Ni side manifested higher hardness.

11. Characterization of Engineered Nickel-Base Alloy Surface Layers Produced by Additive Friction Stir Processing:

Author: J. Rodale's

Materials and tools: A Ni-Cr-Mo superalloy, Haynes Alloy 282, was deposited onto an INCONELTM Alloy 600 (IN600) substrate. IN600 is a solid-solution strengthened alloy that cannot be strengthened by heat treatment. Alloy 282 was chosen based on availability as a welding filler metal and its moderately high Co content, 3.4 wt. %Al. A programmable GTA welding machine was used to deposit Alloy 282. Shallow weld overlays of Alloy 282 were produced on top of IN600 using as welding speed, current, voltage, and wire feed speed of 1.27 mm/s, 105 A, 9.8 V, 6.56 mm/s, respectively. A total of four overlapping passes were approximately 2 mm thick and were placed on top of a 75*9*150 mm IN600 plate that was 6.3 mm thick. This arrangement allowed for a relatively flat deposition surface that could be subsequently FSP without requiring post-deposition machining. FSP of the Alloy 282 deposition layer to create AFSP regions was performed on a gantry-style FSW machine using a water-cooled 19 mm shoulder diameter W-25Re tool. The tool pin was a featureless truncated conical pin 3.2 mm in length, which was sufficient to process the approximately 2 mm thick Alloy 282 weld overlay. Argon shielding was used to minimize oxidation of the workpiece

during AFSP. Physical simulation of the AFSP thermal cycle was performed on as-deposited Alloy 282 weld overlay using 3800 thermo mechanical simulator. Additive FSP samples with and without post-AFSP aging heat treatments were examined using several techniques. The presence of constituent phases within sectioned and polished specimens were selectively etched to reveal precipitates was observed using a high-resolution scanning electron microscopy (HRSEM) equipped with a semi-immersion through lens detector. Samples for transmission electron microscopy (TEM) examination were prepared and extracted using focused ion beam milling and in situ extraction. A scanning transmission electron microscope (STEM) was used for examination of FIB prepared specimens. Microhardness mapping of AFSP regions was performed using an automated hardness tester. A Vickers diamond indenter was used to create arrays of indents using a 300 g applied load. An indent spacing of approximately 250 μm was utilized.

Hard regions in the as-AFSP SZ corresponded to locations within the microstructure containing lamellar distributions of c0 . Thermal simulation of the Alloy 282 weld overlay indicates that c0 forms in the microstructure near the SZ edge where segregation in the weld overlay was only partially homogenized.

conclusion :

Hardness in the additive surface layers was increased as much as 100 HV0.3 relative to Alloy 600 base material. Low-heat input AFSP parameters resulted in most dispersed distribution of Alloy 282 within the SZ as well as the highest hardness of the additive Alloy 282. Electron backscatter diffraction misorientation analyses indicate a higher degree of stored energy in AFSP material processed using low-heat input conditions. The higher stored energy of low-heat input condition likely accounts for observed increase in microhardness and aging response relative to high-heat input AFSP conditions.

12. Microstructure evolution in a single crystal nickel-based superalloy joint by linear friction welding:

Author: Tie Jun Maa

The cast DD6 superalloy with a nominal chemical composition of (wt.%) Ni-4.3Cr-9Co-2Mo-8W-7.5Ta-2Re-0.5Nb-5.6Al-0.006C after heat treatment was used in this work. The specimens were cut to the following dimensions: width of 6.25 mm, length of 19.2 mm and height of 50 mm with the crystal orientation of [011] respect to the oscillation direction, while the welding interface had an area of $6.25 \times 19.2 \text{ mm}$, and the linear friction oscillation was along the length direction. The welding experiments were conducted by the XMH-160LFW machine. Proprietary welding parameters were selected as follows: friction pressure of 160 MPa, frequency and amplitude of oscillation of 35 Hz and 3 mm, respectively. The microstructure of the weld was examined and analysed under an optical microscope (OM), a field emission scanning electron microscope (SEM) with an electron backscatter diffraction (EBSD) system and transmission electron microscope (TEM). The polished metallographic specimens for SEM observation were cut from the weld and etched with a solution of 8 ml of HCl + 12 ml HCO_3^- + 5 ml H_2O_2 . The Vickers microhardness measured using a hardness tester under a load of 500 g for 15 s. The tensile specimens were made and the tensile properties were tested at the Shimadzu AG-X testing machine.

Conclusion: properties due to root defects, i.e. cracks or oxide inclusions. The microstructure at the WZ is polycrystalline instead of a single crystal because of recrystallization. Both elongated and globular γ' phase exist in the TMAZ, the amount of γ' is reduced compared to the PM and shows a maximum at the periphery. The increase in microhardness in the WZ and the TMAZ can be attributed to grain refinement, fine γ' phase and distortion.

13. Surface characterization of Inconel alloy 825 Ni-based alloy / 2507 super duplex stainless steel dissimilar friction stir welds

Author: Jalal Kangazian1

Materials and tools: The base materials were UNS S32750 (SAF 2507) SDSS and UNS N08825 (Inconel alloy 825), with the dimensions of 100 mm × 50 mm × 3 mm. The base metals were then degreased using an acetone solution to remove the contaminants such as rust and grease. The friction stir welding was conducted using a tungsten carbide (WC) tool with the shoulder of 18 mm and the pin diameter of 5 mm. Erstwhile to performing the corrosion tests, the samples were ground up to 1200 grit on Sic papers; then they were polished using alumina powder (0.05 µm).

conclusion :Dynamic recrystallization resulted in fine grain microstructure in stir zone and higher hardness values, as compared to the other zones. The formation of finer grains in the stir zone did not change the pitting corrosion behaviour of stir zone more than the related base metal. In this region, pitting corrosion preferentially occurred in the austenite and austenite grain boundaries. In general, the FSW of SAF 2507 to Incoloy 825 could deteriorate the corrosion properties of the surface.

Over all Conclusion: By studying all those papers we are learned that how much tool rotation speed , how much transverse speed and tilt angle we need to give. For what materials what are the tools we need to use and what are the different types of materials and their alloys are there. How much temperature the materials and tools will sustain. By taking references we are going to initiate our work.

References

- 1.I.A. Choudhury, M.A. El-Bara die, et al ,Machinability of nickel-base super alloys: a general review; School of Mechanical and Manufacturing Engineering, Dublin City University, Glasnevin, Dublin9 , Ireland; Journal of Materials Processing Technology 77 (1998) 278–284.
- 2.P. Mironov, V. N. Grishkov, A. I. Lotkov, V. Yu. Rubtsov, and V. A. Beloborodov, et al, Influence of friction stir processing on the structure and phase state of TiNi alloys,Cite as: AIP Conference Proceedings 2167, 020226 (2019); <https://doi.org/10.1063/1.5132093> Published Online: 19 November 2019Yu.
- 3.R.J. Steel, T.W. Nelson, C.D. Sorensen, Y.S. Sato, C.J. Sterling, and S.M. Packer,et al,Friction Stir Welding of Stainless Steel and Nickel Base Alloys.
- 4.,* Y.G. Zheng, ‡,* S.L. Jiang,* D.R. Ni,** and Z.Y. Ma, et al, Comparison of Corrosion and Cavitation Erosion Behaviours 1 between the As-cast and Friction-stir Processed Nickel 2 Aluminium Bronze 3 .
- 5.Qi Xian Zheng, Xiamen Feng, Yifu Shen, Guoqiang Huang, Pengcheng Zhao,et al, Effect of plunge depth on microstructure and mechanical properties of FSW lap joint between aluminium alloy and nickel-base alloy,PII: S0925-8388(16)33348-5 DOI: 10.1016/j.jallcom.2016.10.213 Reference: JALCOM 39380.
- 6.Rodale's • J. Lippold,etal,Characterization of Engineered Nickel-Base Alloy Surface Layers Produced by Additive Friction Stir Processing. ;SpringerScience Business Media New York and ASM International 2013.
- 7.Jalal KANGAZIAN, Morteza SHAMANIAN,et al, Microstructure and mechanical characterization of Inconel alloy 825 Ni-based alloy welded to 2507 super duplex stainless steel through dissimilar friction stir welding Department of Materials Engineering, Isfahan University of Technology, Isfahan, 8415683111, Iran Trans. Nonferrous Met. Soc. China 29(2019) 1677–1688.
- 8.JAMES R. RULE and JOHN C. LIPPOLD,et al, Friction Stir Welding of Ferrous and Nickel Alloys,Carl D. Sorensen and Tracy W. Nelson Department of Mechanical Engineering, Brigham Young UniversityPhysical Simulation of Friction Stir Welding and Processing of Nickel-Base Alloys Using Hot Torsion;; The Minerals, Metals & Materials Society and ASM International 2013
- 9.Akbar Heidarzadeh, Ali Chabok, Reza Taherzadeh Mousavian & Yutao Pei et al,High-resolution EBSD characterisation of friction stir welded nickel–copper alloy: effect of the initial microstructure on

microstructural evolution and mechanical properties.

10.S.S. Mani Prabu, H.C. Madhu, Chandra S. Perugu, K. Akash, R. Mithun, P. Ajay Kumar, Satish V. Kailas, Manivannan Anbarasu, I.A. Palani, et al, Shape memory effect, temperature distribution and mechanical properties of friction stir welded nitinol.

11.G. V. B. Lemos, S. Hanke, J. F. Dos Santos, L. Bergmann, A. Reguly & T. R. Strohaecker, et al, Progress in friction stir welding of Ni alloys; ISSN: 1362-1718 (Print) 1743-2936 (Online) Journal homepage: <http://www.tandfonline.com/loi/ystw20>.

12.M. Z. Ahmed*1, B. P. Wynne2 and J. P. Martin3, et al, Effect of friction stir welding speed on mechanical properties and microstructure of nickel based super alloy Inconel 718M.

13.Jalal Kangazian1, Morteza Shamanian, Ali Ashrafi, et al, Surface characterization of Inconel alloy 825 Ni-based alloy / 2507 super duplex stainless steel dissimilar friction stir welds Department of Materials Engineering, Isfahan University of Technology, Isfahan, 8415683111, Iran.

14S.S. Mani Prabua,*, Chandra S. Perugub, Madhu H.C.c, Ashutosh Jangdeb, Sohel Khand, S. Jayachandrand, M. Manikandand, P. Ajay Kumare, Satish V. Kailasf, I.A. Palan, et al, Exploring the functional and corrosion behaviour of friction stir welded NiTi shape memory alloy; Contents lists available at ScienceDirect Journal of Manufacturing Processes journal homepage: www.elsevier.com/locate/manpro.

15.S. M. Mousavizade, M. Pouranvari, F. M. Ghaini, H. Fujii & Y. D. Chung, et al, Laser-assisted friction stir processing of IN738LC nickel-based superalloy: stir zone characteristics ISSN: 1362-1718 (Print) 1743-2936 (Online) Journal homepage: <http://www.tandfonline.com/loi/ystw20>.

16.N. Zhang, X. Cao*, S. Larose and P. Wanjara et al, Review of tools for friction stir welding and processing.

17.CARACTERIZAÇÃO DE UMA JUNTA SOLDADA DE INCONEL 625 OBTIDA PELO PROCESSO FRICTIO STIR WELDING

<https://www.researchgate.net/publication/327297570>.

18.Residual stress characterization in friction stir welds of alloy 625 Article in Journal of Materials Research and Technology
<https://www.researchgate.net/publication/333521987>.

19.S.S. Mani Prabua,*, Chandra S. Perugub, Madhu H.C.c, Ashutosh Jangdeb, Sohel Khand, S. Jayachandrand, M. Manikandand, P. Ajay Kumare, Satish V. Kailasf, I.A. Palania, et al, Exploring the functional and corrosion behaviour of friction stir welded NiTi shape memory alloy; journal homepage: www.elsevier.com/locate/manpro.

20.C.G. Rhodes, M.W. Mahoney, W.H. Bingel, R.A. Spurling and C.6. Bampton Rockwell Science Center, Thousand Oaks, CA 91360 ,et al, EFFECTS OF FRICTION STIR WELDING ON MICROSTRUCTURE OF 7075 ALUMINUM.

21.Olga Valerio Flores, Christine Kennedy, L.E. Murr, David Brown, Sridhar Pappu, Brook M. Nowak and J.C. McClure, et al, MICROSTRUCTURAL ISSUES IN A friction stir welding aluminium alloy, Department of Metallurgical and Materials Engineering and Materials, Research Institute, The University of Texas at El Paso, El Paso, TX 79968.

22.I. SHIGEMATSU, Y.-J. KWON, K. SUZUKI, T. IMAI, N. SAITO, et al, Joining of 5083 and 6061 aluminium alloys by friction stir welding, Institute for Structural and Engineering Materials (ISEM), National Institute of Advanced Industrial Science and Technology (AIST), 2266-98, Anagahora, Shimoshidami, Moriyamaku, Nagoya, Aichi 463-8560, Japan.

23.Ulrike Dressler, Gerhard Biallas1, Ulises Alfaro Mercado, et al, Friction stir welding of titanium alloy TiAl6V4 to aluminium alloy AA2024-T3, German Aerospace Centre, Institute of Materials Research, Linder Hohe, 51147 Köln, Germany

24.W.B.Lee, Y.M. Yeon and S.B. Jung, et al, Joint properties of friction stir welded AZ31B–H24 magnesium alloy.

25.Yutaka S. Sato*, Hideaki Takauchi, Seung Hwan C. Park, Hiroyuki Kokawa,et al,Characteristics of the kissing-bond in friction stir welded Al alloy 1050,Department of Materials Processing, Graduate School of Engineering, Tohoku University, 6-6-02 Aramaki-aza-Aoba, Sendai 980-8579, Japan.

26. S.R. Ren, Z.Y. Ma* and L.Q. Chen, etal, Effect of welding parameters on tensile properties and fracture behaviour of friction stir welded Al–Mg–Si alloy.

27.S.Rajakumara,C.Muralidharanb,V.Balasubramaniana,e t al, Influence of friction stir welding process and tool parameters on strength properties of AA7075-T6 aluminium alloy joints, ACenter for Materials Joining & Research (CEMAJOR), Department of Manufacturing Engineering, Annamalai University, Annamalainagar 608 002, Chidambaram, Tamil Nadu, India b)Department of Manufacturing Engineering, Annamalai University, Annamalainagar 608 002, Chidambaram, Tamil Nadu, India.

28.U.F.H.R. Suhuddina, S. Mironova*, Y.S. Satoa, H. Kokawaa, C.-W. Leeb,et al,Grain structure evolution during friction-stir welding of AZ31 magnesium alloy.

29.P. CAVALIERE*,E.CERRI ,et al, Mechanical response of 2024-7075 aluminium alloys joined by Friction Stir WeldingDepartment of “Ingegneria dell’Innovazione,” Engineering Faculty, University of Lecce, Italy E-mail: pasquale.cavaliere@unile.it A. SQUILLACE Department of Materials and Production Engineering, Engineering Faculty, University of Naples Federico II, Italy.

30.SEUNG HWAN C. PARK, YUTAKA S. SATO, HIROYUKI KOKAWA,et al,Microstructural evolution and its effect on Hall-Petch relationship in friction stir welding of thixomolded Mg alloy AZ91D,Department of Materials Processing, Graduate School of Engineering, Tohoku University, Aoba-yama 02, Sendai 980-8579, Japan E-mail: park@stu.material.tohoku.ac.jp.